P1.8 CNR-IMAA LIDAR SYSTEM FOR AEROSOL STUDY: 6 YEARS OF RAMAN MEASUREMENTS

Lucia Mona*, Aldo Amodeo, Carmela Cornacchia, Giuseppe D'Amico, Fabio Madonna, Gelsomina Pappalardo

Istituto di Metodologie per l'Analisi Ambientale CNR-IMAA,
C.da S. Loja,Tito Scalo, Potenza, Italy, I-85050

1. INTRODUCTION

Aerosols effect on the radiation budget is a critical component on global climate, in fact, depending on the aerosol type, they can absorb or scatter the incoming and outgoing radiation, and, depending on their size and composition, they can act as condensation nuclei, modifying cloud physical and radiative properties. The main difficulties in the determination of the direct and indirect effects of aerosols on the Earth's radiative balance are related to the high inhomogeneity and variability of atmospheric aerosol. In particular, the high variability of the tropospheric aerosols, in terms of concentration, shape, size distribution, refractive index and vertical distribution, make the tropospheric aerosols one of the most uncertain elements in the estimation of radiation budget. Long-term measurements of vertical profiles of aerosol optical properties are needed to reduce these uncertainties. At CNR-IMAA (40°36'N, 15°44' E, 760 m above sea level), a lidar system for aerosol study is operative since May 2000, in the framework of EARLINET, the first lidar network for tropospheric aerosol study on continental scale.

2. CNR-IMAA LIDAR SYSTEM

The CNR-IMAA lidar system is a Raman/elastic lidar system based on a Nd:YAG laser equipped with second and third harmonic generators. Since May 2000 until August 2005, the system provided independent measurements of aerosol extinction and backscatter at 355 nm and aerosol backscatter profiles at 532 nm. After then, the CNR-IMAA lidar system for aerosol was upgraded to increase the number of retrievable parameters, in order to obtain more information about microphysical properties of the particles. In particular, since August 2005, this system can provide independent measurements of aerosol extinction and backscatter profiles at 355 and 532 nm, and of aerosol backscatter profiles at 1064 nm. In this way, lidar ratio profiles at 355 and 532 nm and Angstrom exponent profiles at 355/532 nm are obtained. Multi-wavelength measurements (3 backscatter + 2 extinction) allow the determination of microphysical aerosol properties (refractive index, single-scattering albedo and effective particles radii). The high quality of the aerosol optical properties vertical profiles has been demonstrated within the quality assurance exercises performed within EARLINET [Böckmann et al., 2004; Pappalardo et al., 2004a].

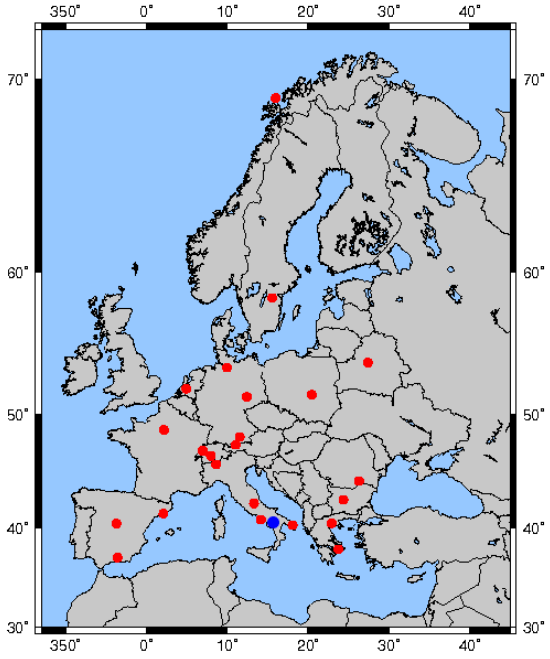

Figure 1: lidar stations of the EARLINET network (red dots). The CNR-IMAA location is indicated as a blue dot.

Two further channels were added at the new CNR-IMAA aerosol lidar to detect the components of backscattered light polarized perpendicular and parallel to the direction of the linearly polarized transmitted laser beam at 532 nm. Starting from these two lidar signals and with the support of the total backscattered signal at 532 nm, depolarization ratio profiles are obtained providing information about shape and orientation of aerosolic particles. This upgraded system is involved in the validation program of aerosol data products from the CALIPSO (Cloud-Aerosol Lidar and Infrared Pathfinder Satellite Observations) satellite mission, providing a reference point for depolarization ratio and aerosol backscatter at 532 and 1064 nm measurements.

* *Corresponding author address*: Lucia Mona, Istituto di Metodologie per l'Analisi Ambientale CNR-IMAA, C.da S. Loja, Tito Scalo, Potenza, Italy, I-85050; e-mail: mona@imaa.cnr.it

3. LONG-TERM MEASUREMENTS

Starting on May 2000, we perform three systematic lidar measurements per week according with the EARLINET schedule. On the base of systematic measurements, a climatological study has been carried out in terms of the seasonal behaviour of the PBL height and of the aerosol optical properties calculated inside the PBL itself. The PBL height is determined out of lidar data by looking at the first significant negative gradient in the range corrected lidar signal, starting from the ground [Matthias et al., 2004]. Following this definition the PBL height is that height below which most of the aerosol is confined and it can include the mixing layer and the residual layer if it exists. An example of determination of the PBL height starting from lidar data is reported in Figure 2. The first panel on the left reports the aerosol backscatter and extinction profiles, that show a sharp decrease in the aerosol load at about 1.5 km above the lidar station. In the second panel the lidar range corrected signal and its first derivate are reported. The latest has a first minimum around 1km a.l.s. and a second minimum around 1.5 km, which identify the lower and upper limits of the residual layer. The third panel reports the potential temperature (Tpot) and the relative humidity (RH) profiles provided by a radiosonde, launched on September 18, 2002 at 20:32 UT, simultaneously to the lidar measurement. Both potential temperature and relative humidity profiles present a strong gradient around the determined PBL height. Finally the panel on the right of Figure 2 reports the lidar ratio vertical profile: the lidar ratio value increases with the altitude from the first point up to the PBL top (1.5 km), probably because of relative humidity increase. At higher altitude the lidar ratio is almost constant around a value close to 50 sr.

All aerosol optical parameters integrated on the PBL show a significant seasonal dependence, lidar ratio at 355 nm instead does not depend on the season. The absence of significant differences between mean lidar ratio observed in winter and summer could indicate that, on average, the mixture of local aerosol confined in the PBL is the same for all the year. The mean lidar ratio values observed in the PBL are distributed following a single mode Gaussian distribution reported in Figure 3. Lidar ratio PBL mean values range between a minimum of 10.2 sr to a maximum of 83.4 sr with rapid changes from day to day, due to the natural variability of the aerosol optical properties. Nevertheless, the distribution of measured mean values show that these values are distributed around a central value of 37 sr.

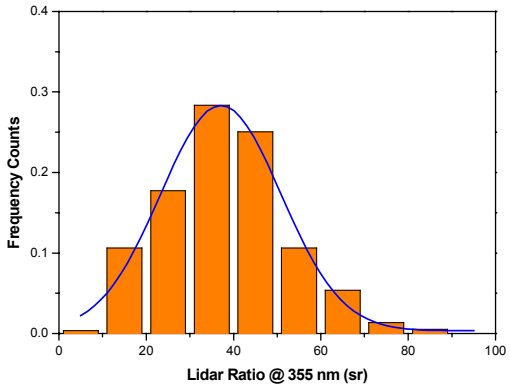

Figure 3: Frequency count distribution of lidar ratio mean values calculated in the PBL (orange bar) and Gaussian fitting curve (blue line).

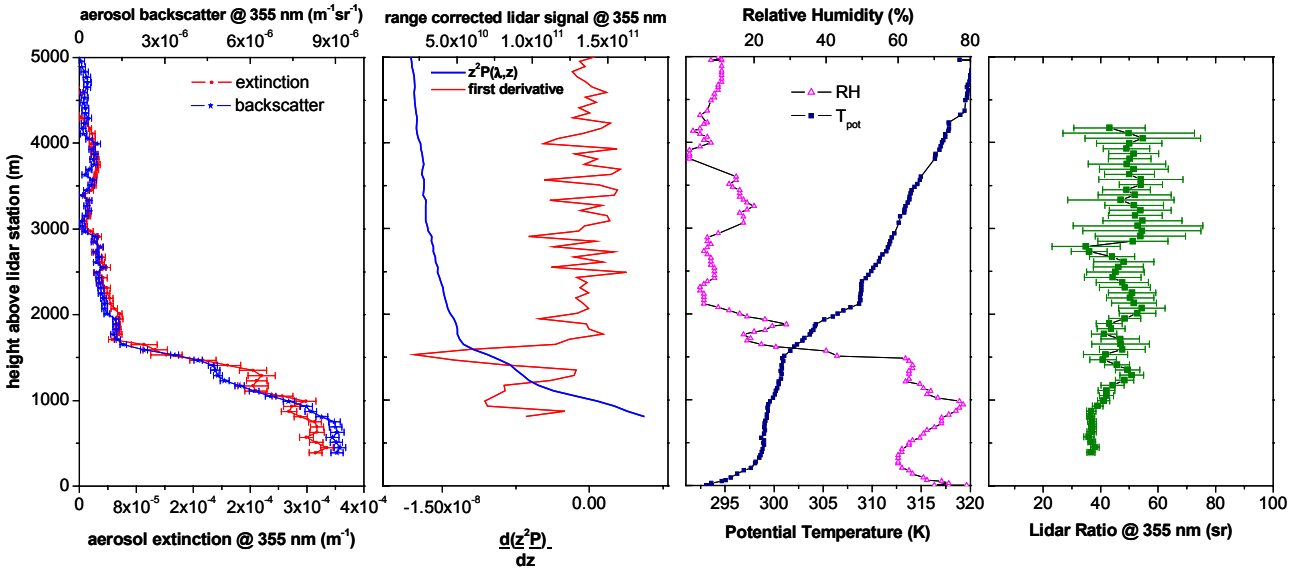

Figure 2: determination of PBL height with lidar data (September 18, 2002 (20:30-20:45 UT)) and comparison with simultaneous and co-located radiosounding (September 18, 2002 at 20:32 UT).

Further measurements are performed in order to investigate particular events, like dust intrusions, volcanic eruptions and forest fires. Among cases with aerosol layer above the PBL, cases of Saharan dust intrusions at our site are identified by means of backtrajectories analysis and in accordance with satellite images. Because of the short distance between our site and the Sahara desert, about 1 day of Saharan dust intrusion every 10 days is observed [Mona et al., 2006]. The Saharan dust layers are observed between 1.8 and 9 km. A mean optical depth of 0.13 is observed inside the Saharan dust layer, reaching a maximum value of 0.68.

Starting from our observations, three main source regions for Saharan dust (Figure 4) are identified by means of DWD backward trajectories analysis. The source origin is the central Sahara in about 66% of the cases, the western Sahara in about 30%, and only in 4 cases the eastern Sahara.

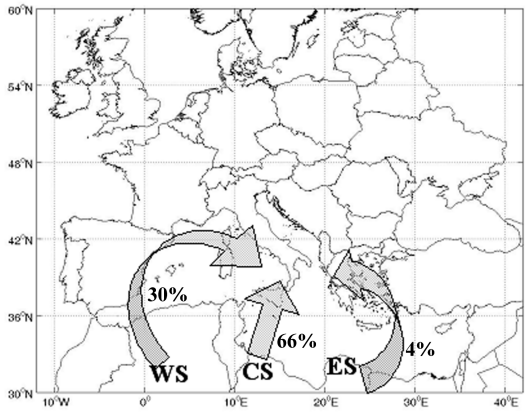

Figure 4: dust origin for Saharan dust observed at CNR-IMAA. The arrows show typical paths. Also the percentages of cases for the different origins are reported.

A wide range of values is observed for lidar ratio at 355 nm collected in the desert dust layer, as shown in the frequency counts distribution reported in Figure 5 in 10 sr bins (black squares). The experimental distribution is well fitted (correlation coefficient 0.997) by a tri-modal Gaussian distribution (red line) that is the sum of three Gaussian distributions (blue lines) centered around 22 sr (mode a), 37 sr (mode b) and 57 sr (mode c). A climatological analysis based on the large database of collected Saharan dust data allowed the physical interpretation of each one of these modes [Mona et al., 2006]. In particular, the low observed lidar ratio mode (mode (a)) is related to the cases in which a large amount of dust is transported at low altitudes over the Mediterranean Sea, with a consequent contamination between desert dust and maritime aerosols. The mode (b) centered around 37 sr comes out from the core of Saharan dust layer, so that it can be representative of pure Saharan dust, in perfect agreement with theoretical values reported in the literature [Ackermann, 1998].

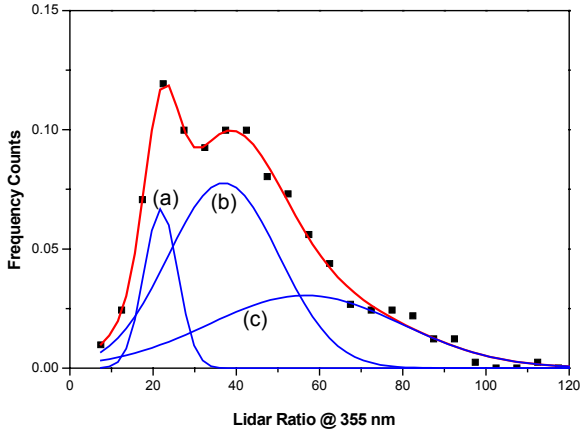

Figure 5: frequency count distribution for lidar ratio values collected in the desert dust layer (black squares) and best fitting 3-modal Gaussian curve (red line), that is the sum of the 3 gaussian distribution (blue lines).

During these 6 years of observations, very peculiar cases of volcanic aerosol emitted during Etna eruptions in summer 2001 and autumn 2002 have been observed at CNR-IMAA. Figure 6 shows the aerosol backscatter at 532 nm measured at CNR-IMAA on 1-2 November 2002. A strong aerosol layer is evident at 6 km at the beginning of the record and at 4 km around noon on 2 November. A further volcanic layer is observed just above this pronounced layer, that has the same temporal behaviour of the first one. On 1-2 November fast and direct transport from volcano to lidar site occurred, while in previous days aerosol emitted by Etna experienced along path travel before reaching Potenza [Pappalardo et al., 2004b; Villani et al., 2006].

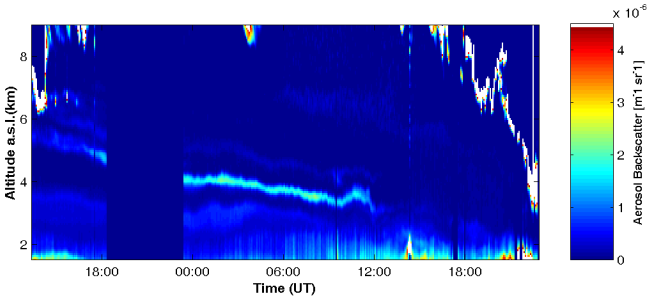

Figure 6: temporal evolution of aerosol backscatter coefficient at 532 nm measured at CNR-IMAA on 1-2 November 2002.

An example of aerosol backscatter and lidar ratio profiles measured at 355 nm for long path transport (on 31st October) and direct transport (1st November) are reported in Figure 7. Mean lidar ratios for the two days are almost equal (53 and 55 sr). But in the case

of direct and fast transport toward our site, lidar ratio is almost constant within the volcanic aerosol layer (4-4.5 km a.s.l.), while a large variability is observed on 31st October in the volcanic aerosol layer extending between 3.2 –5.5 km a.s.l.. The significant difference in lidar ratio variability inside the volcanic aerosol layer can be related to a longer travelled path during which the chemical-physical properties of these particles were modified.

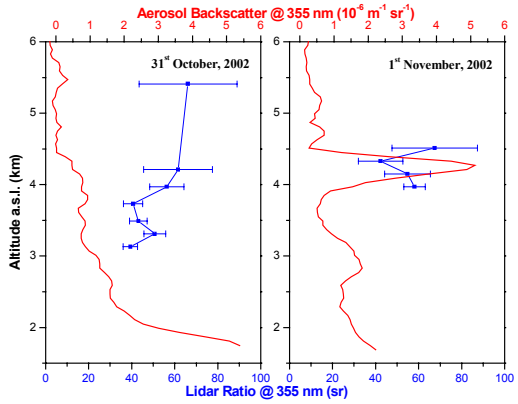

Figure 7. Aerosol backscatter (red lines) and lidar ratio (blue lines) profiles measured at 355 nm on 31st October and 1st November 2002. Lidar ratio profiles inside the identified volcano aerosol layer are also reported with the statistical errors (error bars).

Connections between lidar ratio variability with aerosol modification and mixing were observed also during summer 2004, when we observed aerosol load in the free troposphere related to large forest fires burning occurred in Alaska and in the frame of ICARTT campaign.

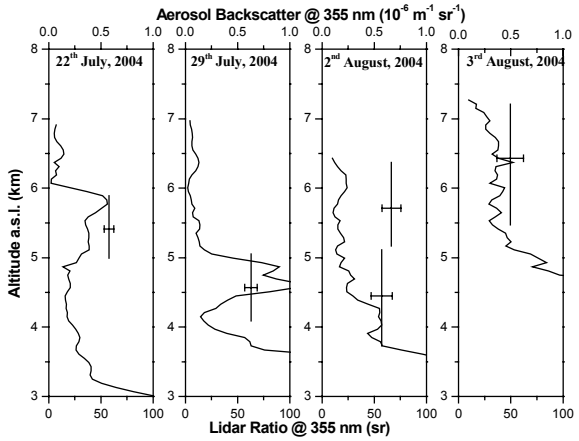

Figure 8: Alaska forest fires observation in summer 2004. Aerosol backscatter profiles at 355 nm (lines); aerosol layer altitude ranges (vertical bars); lidar ratio mean values and its standard deviation in the aerosol layer (point and error bars).

Aerosol backscatter profiles and lidar ratio mean value and standard deviation calculated within the free troposphere aerosol layer are reported in Figure 8 for the period 22 July-03 August, 2004. In the aerosol layer altitude, indicated by the vertical bars, mean lidar ratio and its standard deviation (error bars) range between 50-66 sr, and 4.5-12.5 sr, respectively. In particular, the lidar ratio variability inside the layer is higher when the aerosol layer is lower in altitude and on 3rd August when Saharan dust particles are transported over Europe, i.e. large lidar ratio variability is observed in cases characterized by mixing with local aerosol and desert dust.

ACKNOWLEDGMENT

The financial support of this work by the European Commission under grant RICA-025991 is gratefully acknowledged. The authors also thank the German Weather Service for the air mass backtrajectory analysis.

REFERENCES

Ackermann J., The extinction-to-backscatter ratio of tropospheric aerosol: A numerical study, Journal of atmospheric and oceanic technology, 15, 1043-1050, 1998.

Böckmann, C. et al., Aerosol lidar intercomparison in the framework of EARLINET. 2. Aerosol backscatter algorithms, Appl. Opt., 43, 4, 977-989, 2004.

Matthias, V. et al., The vertical aerosol distribution over Europe: statistical analysis of Raman lidar data from 10 EARLINET stations, J. Geophys. Res., 109, D18201, doi:10.1029/2004JD004638, 2004.

Mona L., et al., Saharan dust intrusions in the Mediterranean area: three years of Raman lidar measurements, accepted for publication on J. Geophys. Res., 2006.

Pappalardo, G., et al., One year of tropospheric lidar measurements of aerosol extinction and backscatter, Ann. Geophys., 46, 401-413, 2003.

Pappalardo, G. et al., Aerosol lidar intercomparison in the framework of EARLINET. 3. Raman lidar algorithm for aerosol extinction, backscatter and lidar ratio, Appl. Opt., 43, 5370-5385, 2004a.

Pappalardo, G. et al., Raman lidar observations of aerosol emitted during the 2002 Etna eruption, Geophys. Res. Lett., 31, L05120, doi:10.1029/2003GL019073, 2004b.

Villani, M.G. et al., Transport of volcanic aerosol in the troposphere: The case study of the 2002 Etna plume, J. Geophys. Res., 111, D21102, doi:10.1029/2006JD007126.